Supplementary Information (SI) for Journal of Materials Chemistry A.

Supporting Information for

Discerning Morphological Evolution Under Thermal Stress in Polymerized Small Molecular Acceptor-based All Polymer Solar Cells

Yuxiang Li,[1]* Yingfan Du,[1] Haim Kwon,[2] Songqiao Li,[3] Pingping Zhang,[1] Min Hun Jee,[2] Tao Sun,[1] Jing Guo,[1] Hongmei Qin,[1] Guanghao Lu,[3] Wenyan Su,[1]* Han Young Woo[2]*

[1]Y. Du, P. Zhang, T. Sun, J. Guo, H. Qin, W. Su, Y. Li
School of Materials Science and Engineering, Xi'an University of Science and Technology, Xi'an 710054, China.
E-mail: suwy1027@xust.edu.cn; liyuxianggj687@xust.edu.cn

[2]H. Kwon, M. H. Jee, H. Y. Woo
Department of Chemistry, Korea University, Seoul 02841, Republic of Korea
E-mail: hywoo@korea.ac.kr

[3]S. Li, G. Lu
Frontier Institute of Science and Technology, Xi'an Jiaotong University, Xi'an 710049, China

1. Materials

Polymer donor PTQ10 and PM6 were purchased from Solarmer Beijing Inc., PBQX-TF was purchased from Derthon Optoelectronics Materials Science Technology Co., Ltd., PTVT-T, D18, and polymer acceptor PY-IT were purchased from Jiaxing Hepu Optoelectronic Technology Co., Ltd., PDINN was purchased from Solarmer Material Inc., and PEDOT: PSS 4083 was commercially available from Heraeus, respectively. MoO_3 was purchased from Solarmer Material Inc., and ZnO was synthesized following the reported synthesis procedure.[1]

The ZnO precursor solution was prepared by dissolving zinc acetate dihydrate ($Zn(CH_3COO)_2 \cdot 2H_2O$, Aldrich, 99.9%, 1g) and ethanolamine ($NH_2CH_2CH_2OH$, Aldrich, 99.5%, 0.28 g) in 2-methoxyethanol ($CH_3OCH_2CH_2OH$, Aldrich, 99.8%, 10 mL) under vigorous stirring. The solutions were stirred for three hours on a hot plate at 60 °C until becoming clear. Before spin-coating, the ITO substrates were treated with oxygen plasma for 10 minutes. Then, the ZnO precursor solution was spin-coated at 4000 rpm for 60 seconds onto the ITO substrates and annealed at 200 °C for 60 minutes in air. During the coating process, the temperature and humidity ranged from 20-25 °C and 30-40%, respectively.

2. Device Fabrication

The patterned indium tin oxide (ITO, Advanced Election Technology Co., Ltd.) coated glass substrates (15 Ω per square) were cleaned via sequential sonication in detergent, deionized water, and isopropanol and then blow-dried by high-purity nitrogen. All pre-cleaned ITO substrates were treated by oxygen plasma for 10 minutes to improve their work function and clearance. Subsequently, poly(3,4-ethylenedioxythiophene): poly (styrene sulfonate) (PEDOT: PSS) solution was spin-coated on ITO substrates at 4500 rpm for 40 s and dried at 150 °C for 15 min in atmospheric air. Then ITO substrates coated with PEDOT: PSS films were transferred into a high-purity N_2-filled glove box. For all-PSCs based on PTQ10:PY-IT blend, the optimal conditions were a D/A weight ratio of 1:1.2, CF as the solvent (PTQ10 concentration was fixed at 7 mg mL^{-1}) with the addition of 1.5% v/v 1-phenylnaphthalene (1-PN). For all-PSCs based on PTVT-

T:PY-IT blend, the optimal conditions were a D/A weight ratio of 1:1.2, CF as the solvent (PTVT-T concentration was fixed at 5.45 mg mL^{-1}) with the addition of 1.5% v/v 1-phenylnaphthalene (1-PN). For all-PSCs based on PM6:PY-IT blend, the optimal conditions were a D/A weight ratio of 1:1.2, CF as the solvent (PM6 concentration was fixed at 7 mg mL^{-1}) with the addition of 1.5% v/v 1-chloronaphthalene (1-CN). For all-PSCs based on D18:PY-IT blend, the optimal conditions were a D/A weight ratio of 1:1, CF as the solvent (D18 concentration was fixed at 4.5 mg mL^{-1}) with the addition of 1% v/v 1-phenylnaphthalene (1-PN). For all-PSCs based on PBQX-TF:PY-IT blend, the optimal conditions were a D/A weight ratio of 1:1.2, CF as the solvent (PBQX-TF concentration was fixed at 5 mg mL^{-1}) with the addition of 1.5% v/v 1-phenylnaphthalene (1-PN). The active layer thicknesses were ~100 nm, measured by a KLA Tencor D-100 profilometer. For all types of devices, a methanol solution of PDINN at a concentration of 1 mg mL^{-1} was spin-coated onto the photoactive layer at 3000 r.p.m. for 30 s. Finally, a 150 nm Ag layer was deposited by thermal evaporation through a shadow mask under a vacuum of 3×10^{-4} Pa conditions.

3. Device Charaterization

The current density-voltage *(J-V)* curves of OSCs were measured using a Keysight B2901A Source Meter in the glove box under AM 1.5G (100 mW cm^{-2}) using an Enlitech solar simulator. The device contact area was 0.04 cm^2. The EQE spectra were measured using a Solar Cell Spectral Response Measurement System QE-R3011 (Enlitech Co., Ltd.). The light intensity at each wavelength was calibrated using a standard monocrystalline Si photovoltaic cell.

For the neat films, polymer solutions were prepared by dissolving PTVT-T, PM6, PTQ10, and D18 in chloroform at a concentration of 10 mg/mL, PBQX-TF in chlorobenzene at 10 mg/mL, and PY-IT in chloroform at 15 mg/mL. For the blend films, the solutions were prepared by carefully controlling the D/A weight ratio, solvent, and post-annealing conditions, identical to those used in device fabrication. For spin-coating, all neat films were deposited at 2000 rpm for 40 seconds to ensure consistent film thickness. To ensure the reliability of the results, the blend films were prepared under the same conditions as the active layers used in devices. The resulting samples were placed on a heating stage and annealed in the dark inside the glove box to replicate the thermal treatment used during device fabrication. UV–vis absorption spectra of both neat and blend films were periodically measured outside the glove box. The photophysical properties were characterized by UV-visible-NIR spectroscopy (Shimadzu 2600i spectrophotometer).

Samples with the structure ITO/PEDOT:PSS/active layer (blend or neat polymer donor/acceptor films) for AFM measurements were prepared following the same procedure as device fabrication. AFM (XE-100, PSIA) in tapping mode was then used for characterization.

Two-dimensional grazing incidence wide-angle X-ray scattering (2D-GIWAXS) measurements were performed at the 9A U-SAXS beamline of the Pohang Accelerator Laboratory (PAL), Republic of Korea, with a beam energy of 11.06 keV and incident angles of 0.12°.[2]

Samples with the structure ITO/PEDOT:PSS/active layer (blend or neat polymer donor/acceptor films) for FLAS measurements were prepared following the same procedure as device fabrication. FLAS measurements were conducted through oxygen plasma etching. The oxygen plasma pressure was kept below 20 Pa during etching to guarantee surface-selective etching without subsurface damage.[3]

Samples with the structures ITO/ZnO/BHJ and ITO/PEDOT:PSS/BHJ were prepared following the same procedure used for device fabrication. These samples were subjected to continuous thermal annealing at 80 °C in a nitrogen atmosphere under dark conditions. After annealing, electrodes were evaporated onto the devices, and their exciton dissociation efficiency and carrier mobility were characterized. By maintaining consistent annealing conditions, the evolution of charge transport performance in the active layer during thermal aging could be precisely monitored.

Hole-and electron-only devices

The hole mobility was measured in a hole-only device composed of ITO/PEDOT:PSS/active layer/MoO_3/Ag. The electron mobility was measured in an electron-only device comprising ITO/ZnO/active layer/PDINN/Ag. The active layers were spin-coated on ITO substrates covered with 40 nm PEDOT:PSS for the hole-only device. The fresh or aged active layers were prepared according to the abovementioned fabrication process of the all-PSCs. After that, MoO_3 (8 nm) and Ag (150 nm) were vacuum-deposited on the active layer as the cathode. For the electron-only device, the blend films were spin-coated on ITO substrates covered with a layer of ZnO (40 nm). The active layers and PDINN were prepared according to the fabrication process of the all-PSCs. After that, Ag (150 nm) was vacuum-deposited on the active layer as the cathode. The charge mobility was determined by fitting the dark current to the space-charge-limit current (SCLC) model of a single carrier SCLC, described by the Equation:

$$J = \frac{9\varepsilon_0\varepsilon_r\mu\left(V_a - V_{bi}\right)^2}{8L^3}$$

Where J is the current density of the hole-only or electron-only devices, ε_0 is the permittivity of free space, ε_r is the relative permittivity of the material, μ is the mobility, V_a is the applied voltage, V_{bi} is the built-in voltage, and L is the thickness of the active layer.[4]

Exciton and carrier dynamics measurements

Exciton dissociation efficiency and charge collection efficiency measurements: J_{ph} is defined as $J_{ph} = J_{light} - J_{dark}$, where J_{light} and J_{dark} are the photocurrent densities under illumination and in the dark, respectively. V_{eff} is defined as $V_{eff} = V_0 - V_a$, where V_0 is the voltage when J_{ph} is 0, and V_a is the applied voltage. J_{ph} corresponding to the maximum V_{eff} is defined as the saturation current (J_{sat}) value. Exciton dissociation efficiency (P_{diss}) is the J_{ph}/J_{sat} value under short-circuit conditions.[5]

Analysis of light intensity dependent J_{SC} and V_{OC}

The relationship between J_{SC} and P_{light} (light intensity) follows the formula of $J_{sc} \propto P_{light}^{S}$. $S = 1$ means the extreme case where all the free carriers are swept out and collected at the corresponding electrodes before recombination, and $S < 1$ implies the existence of bimolecular recombination. Given the relationship of $V_{OC} \propto (nkT/q)\ln(P_{light})$, a slope of kT/q suggests only bimolecular charge recombination, but a slope higher than kT/q suggests defect-mediated recombination.[6]

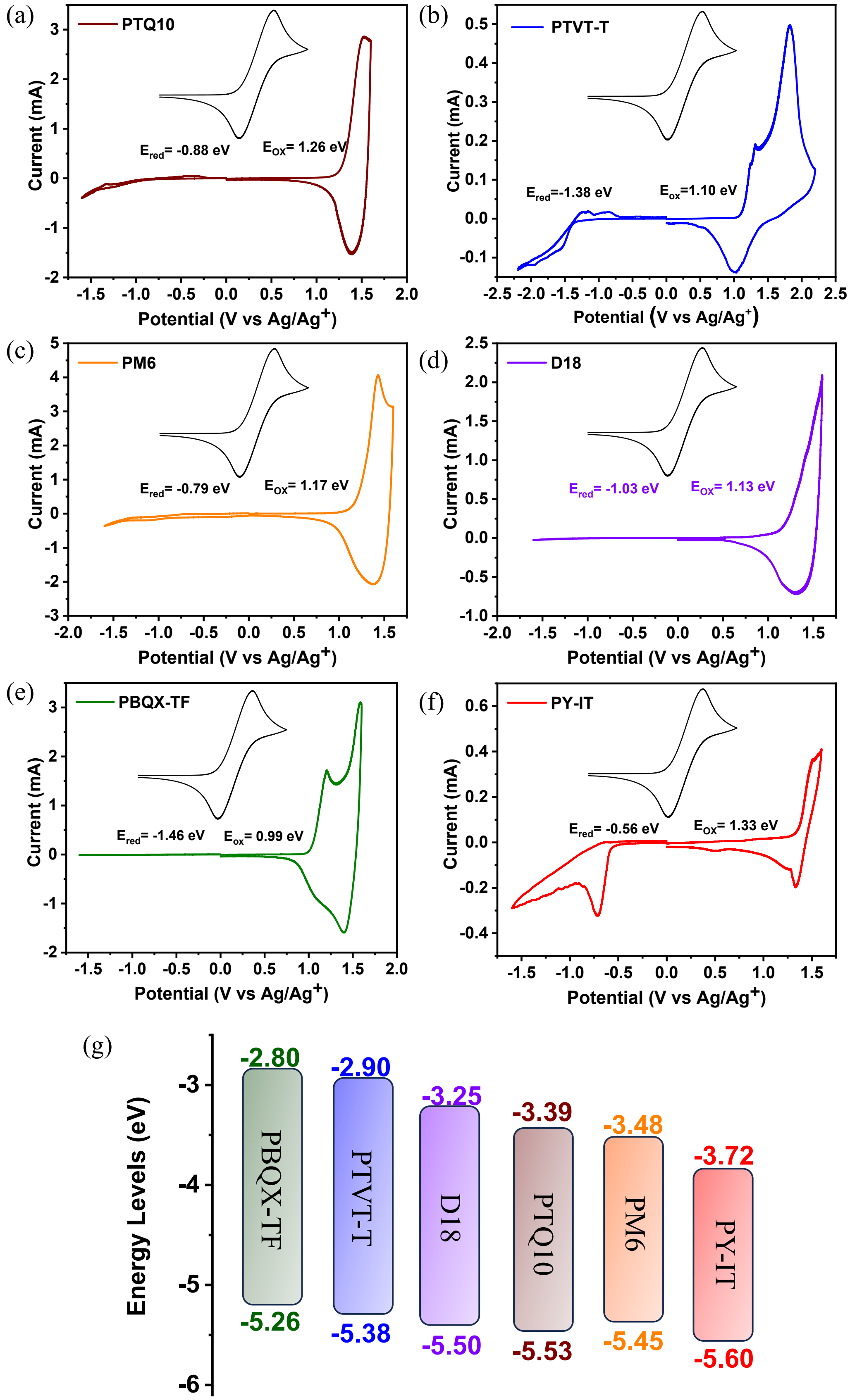

Fig. S1. The CV curves (a-f) and energy level diagram (g) of five polymer donors and PY-IT.

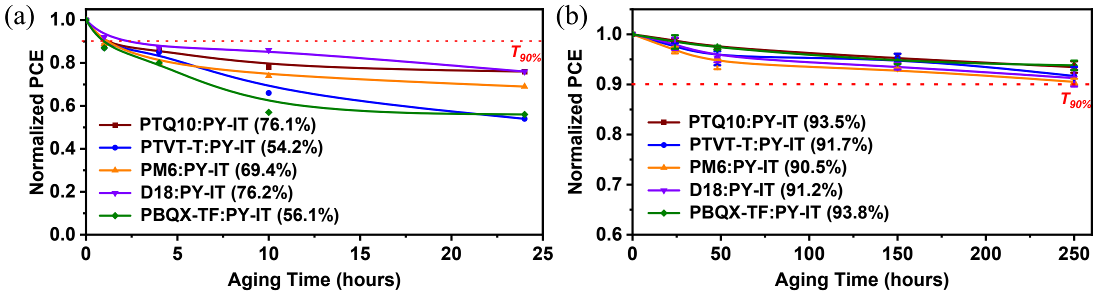

Fig. S2. Variation of normalized PCE of five all-PSC devices as a function of the annealing time of (a) complete devices and (b) active layer under continuous thermal annealing at 80 °C in a nitrogen atmosphere under the dark condition.

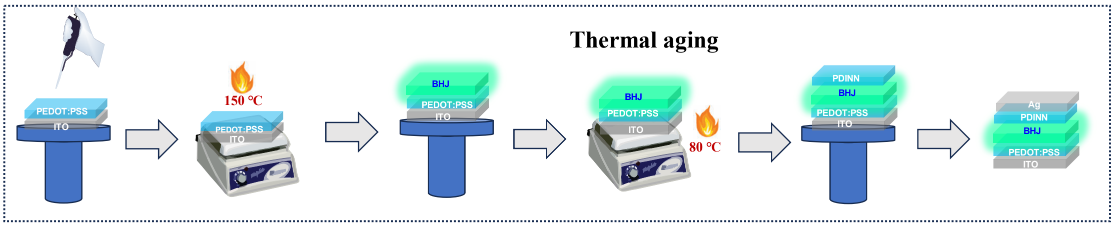

Fig. S3. Schematic illustration of device fabrication procedure.

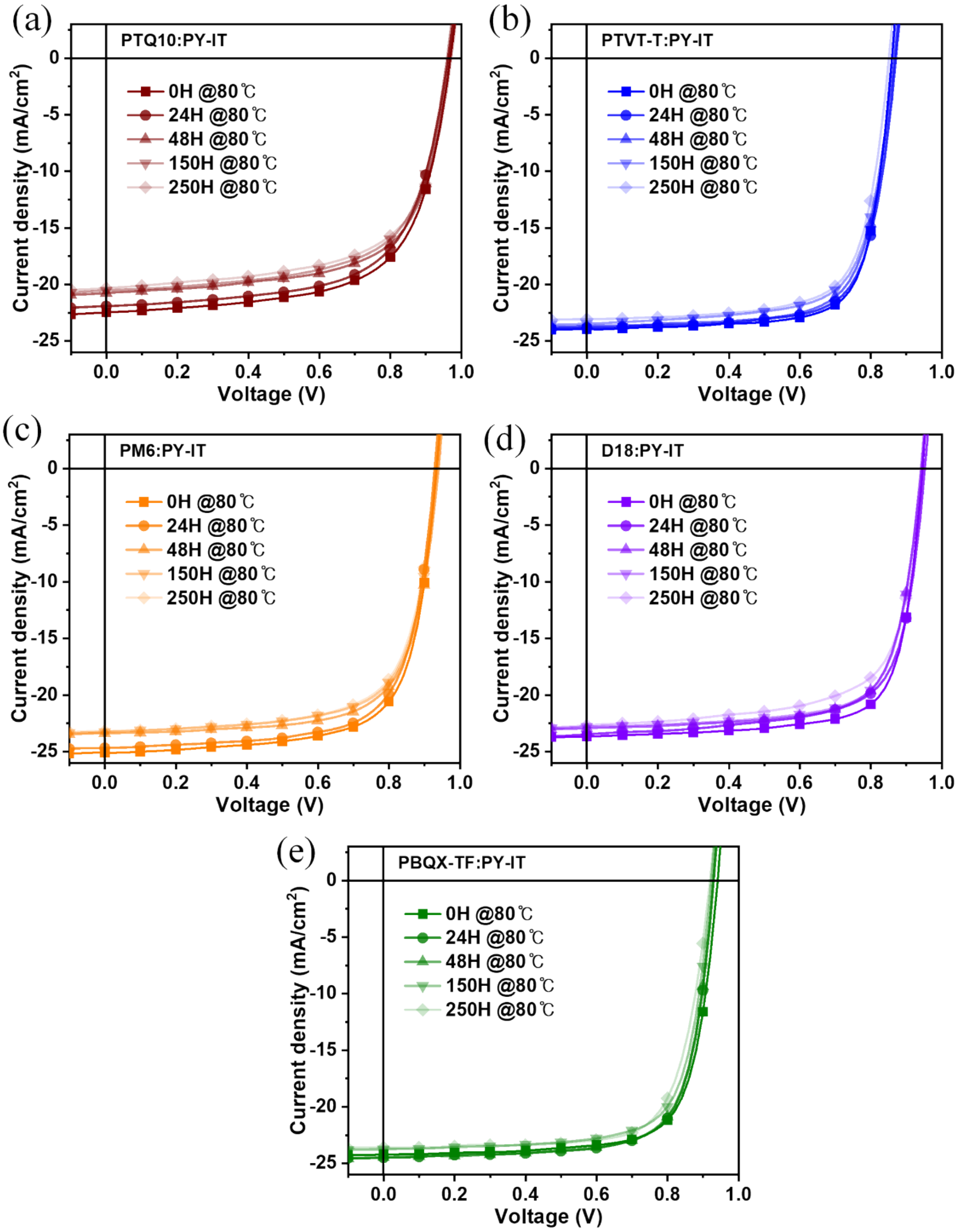

Fig. S4. *J*-*V* curves of (a) PTQ10:PY-IT, (b) PTVT-T:PY-IT, (c) PM6:PY-IT, (d) D18:PY-IT, and (e) PBQX-TF: PY-IT-based all-PSCs based on the different aging times at 80 ℃ in a nitrogen atmosphere under dark conditions.

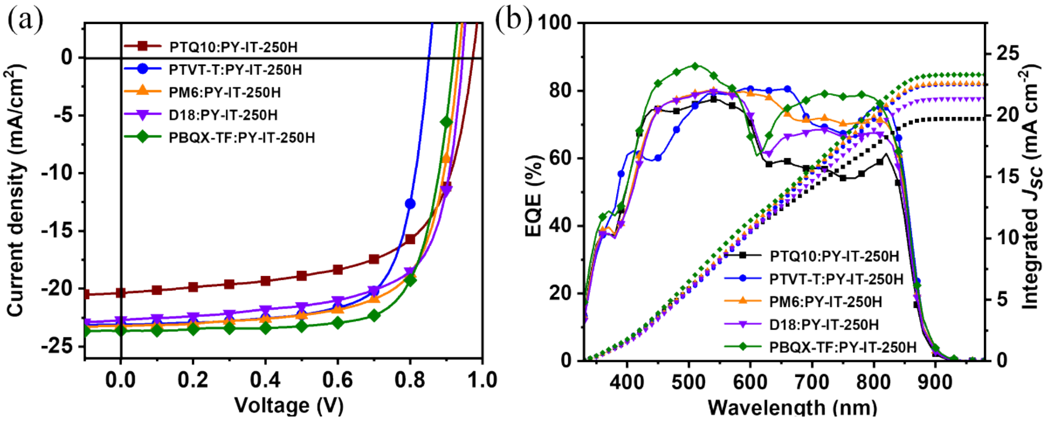

Fig. S5. (a) *J-V* curves and (b) EQE spectra of five PY-IT-based all-PSC devices after thermal treatments at 80 ℃ for 250 hours.

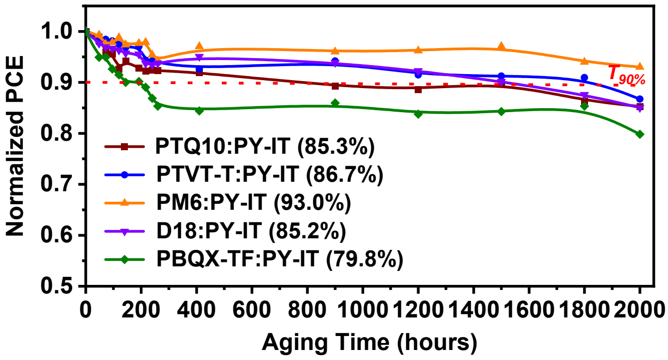

Fig. S6. Variation in normalized PCE for five all-PSC devices during storage under dark conditions in a nitrogen atmosphere.

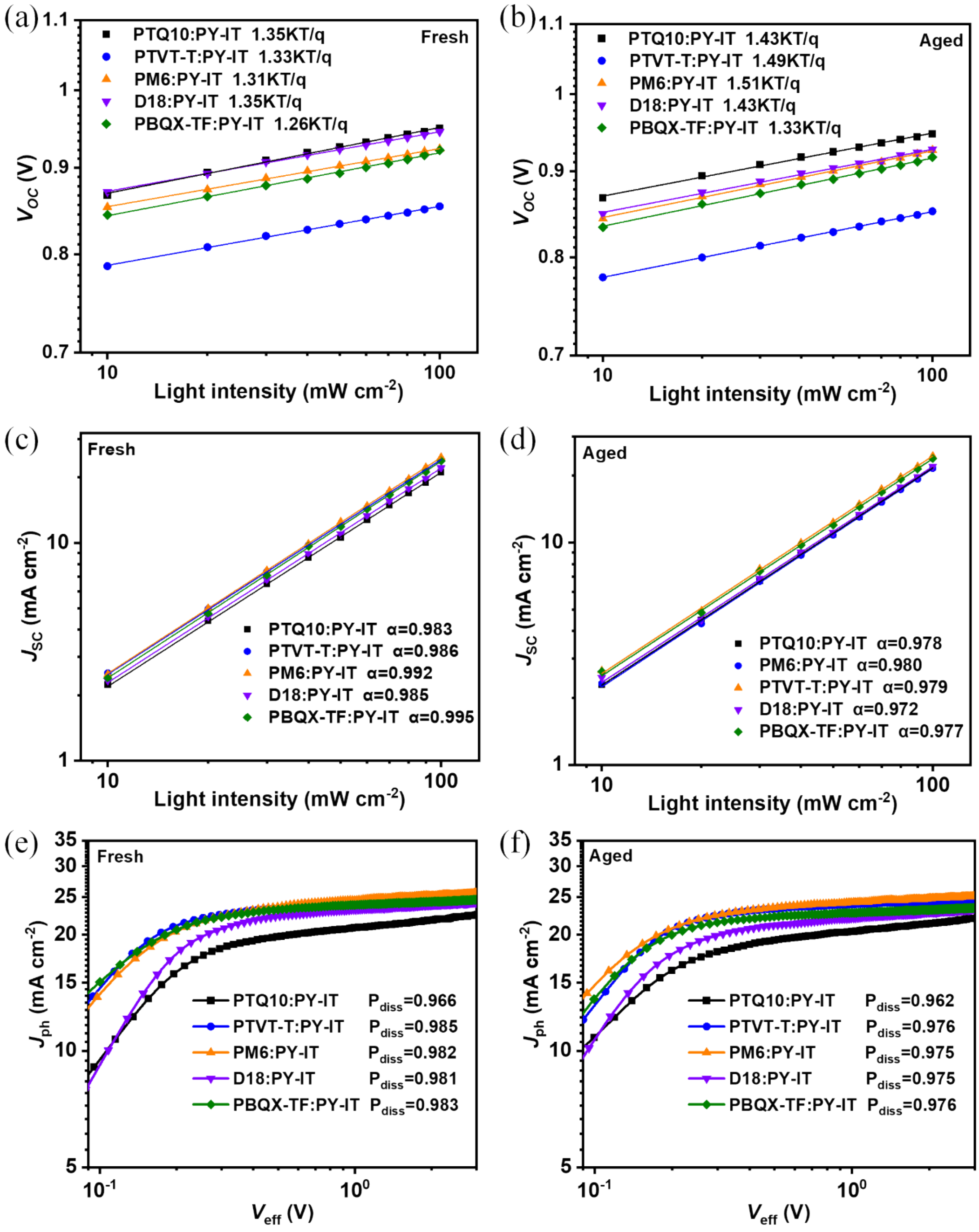

Fig. S7. Light intensity dependent V_{OC} (a, b) and J_{SC} (c, d), along with the J_{ph}-V_{eff} curves (e, f) for fresh and aged devices at 80 °C for 250 hours in nitrogen.

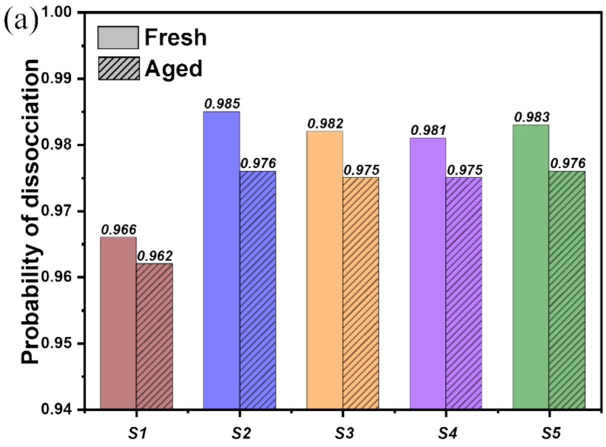

Fig. S8. Variation in P_{diss} of five all-PSC devices before and after thermal treatments at 80 °C for 250 hours (S1: PTQ10:PY-IT, S2: PTVT-T:PY-IT, S3: PM6:PY-IT, S4: D18:PY-IT and S5: PBQX-TF:PY-IT).

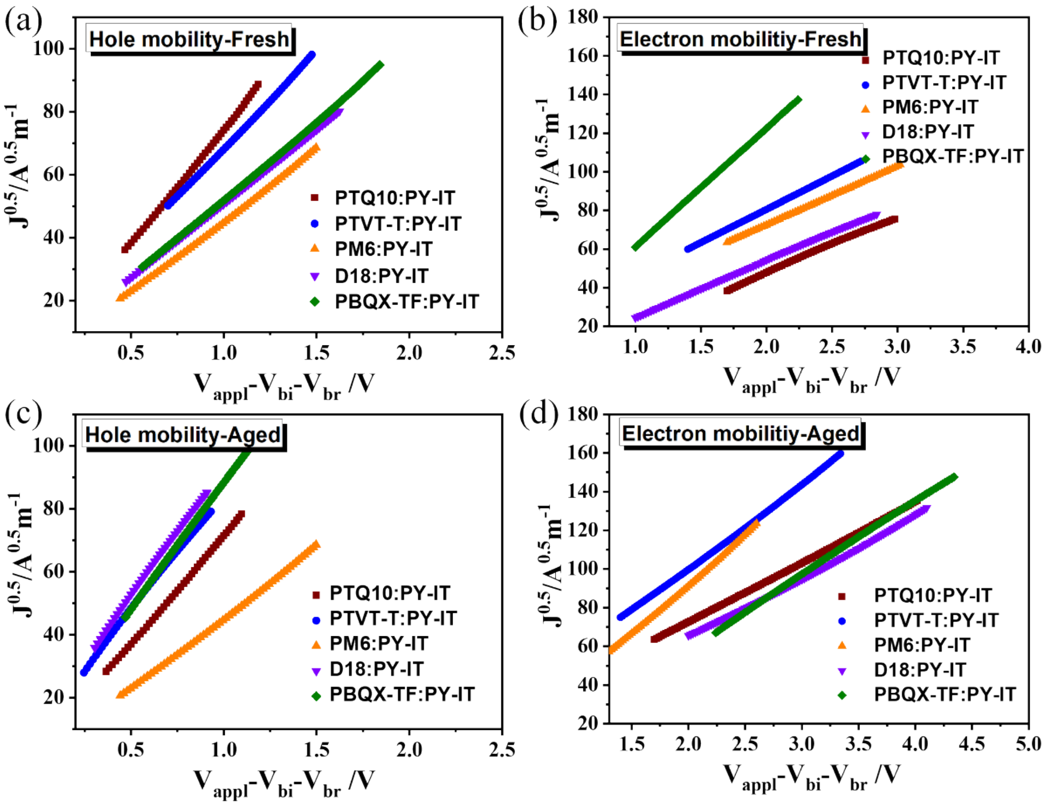

Fig. S9. Determination of hole and electron mobilities of fresh (a, b) and aged (c, d) blend films at 80 °C for 250 hours in nitrogen.

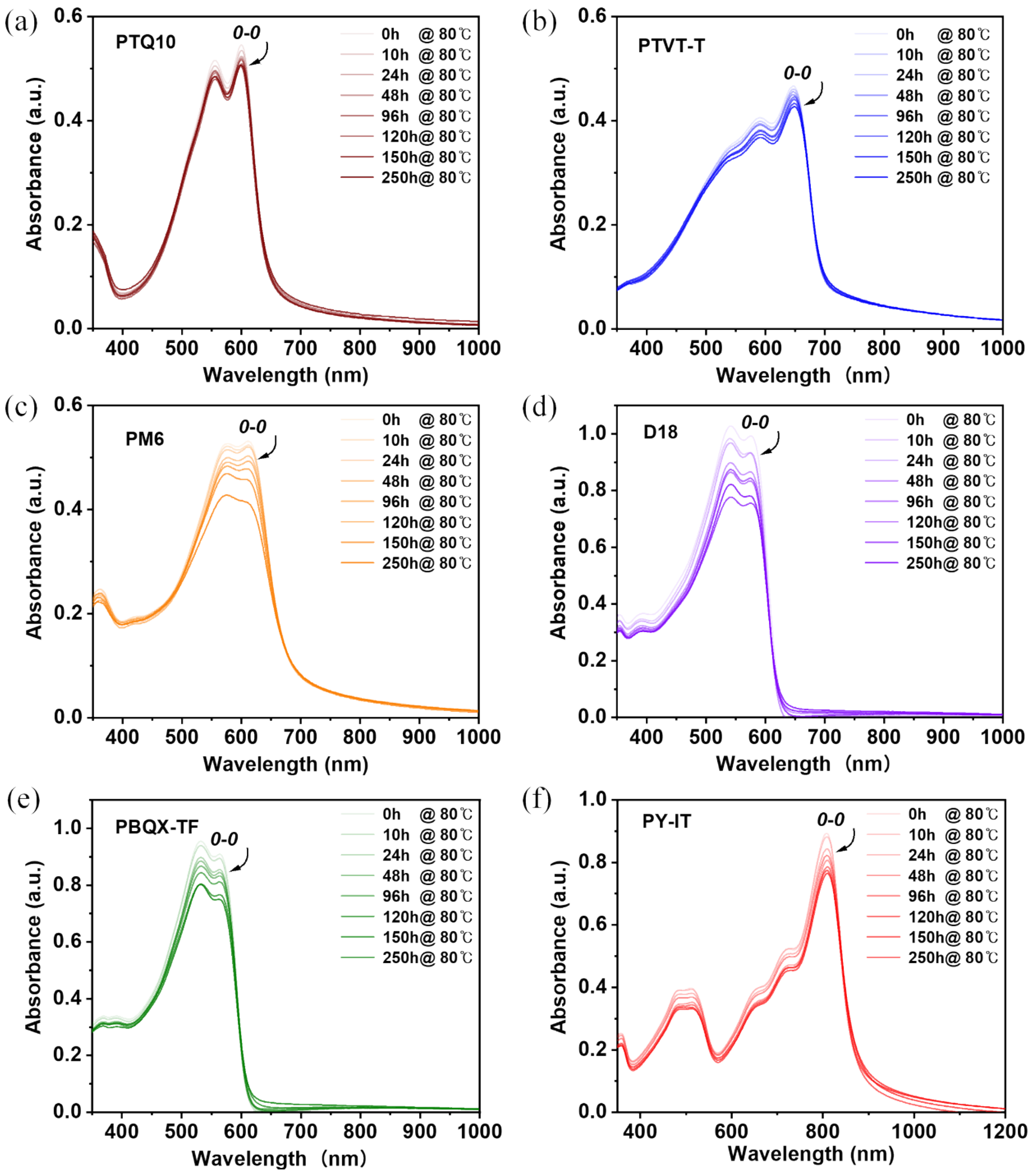

Fig. S10. Absorption spectral changes in the marked *0-0* peaks of five polymer donors (a-e) and PY-IT (f) films with continuous annealing at 80 °C for 250 h.

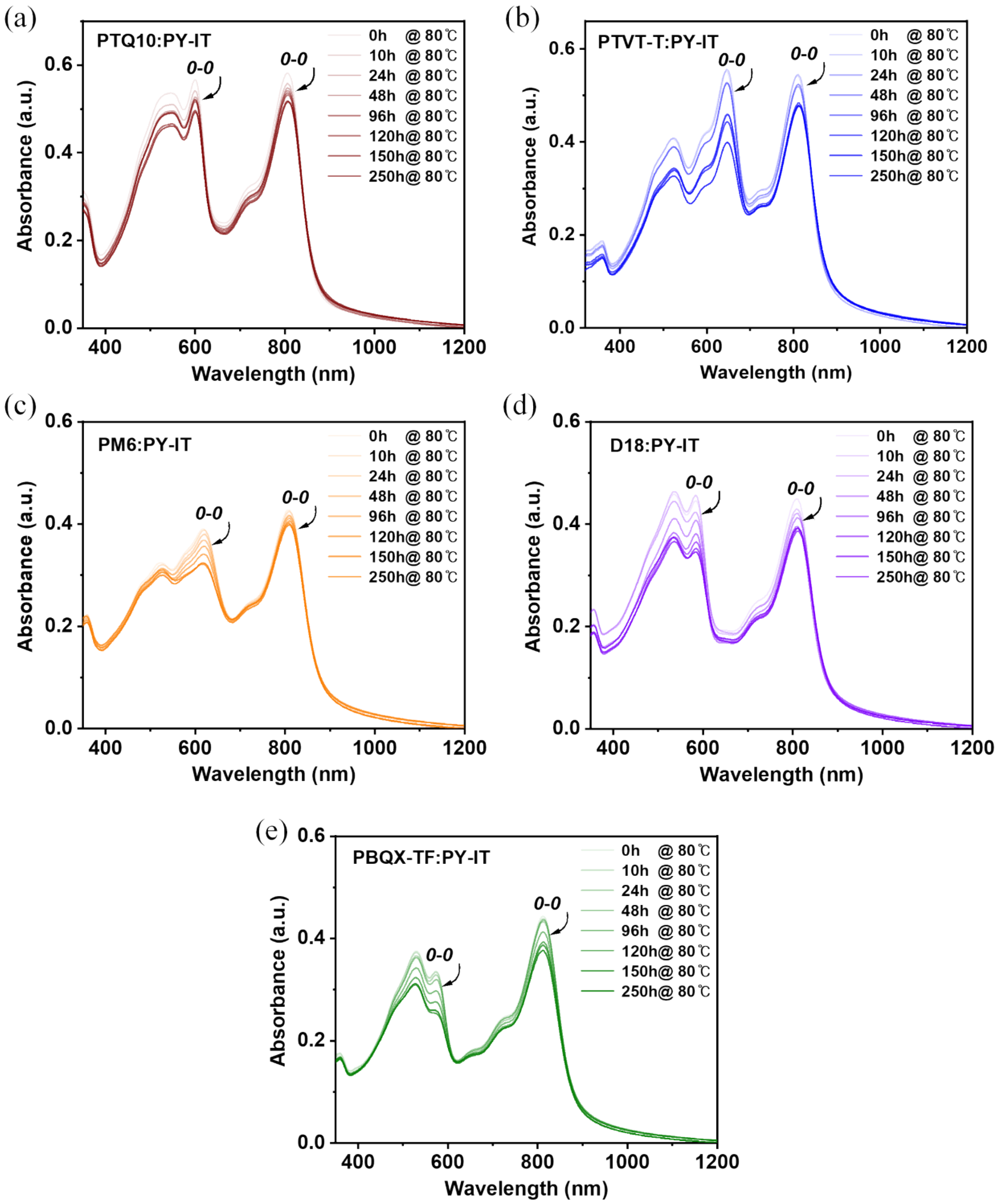

Fig. S11. Absorption spectral changes in the marked *0-0* peaks of blend films (a-f) with continuous annealing at 80 °C for 250 h.

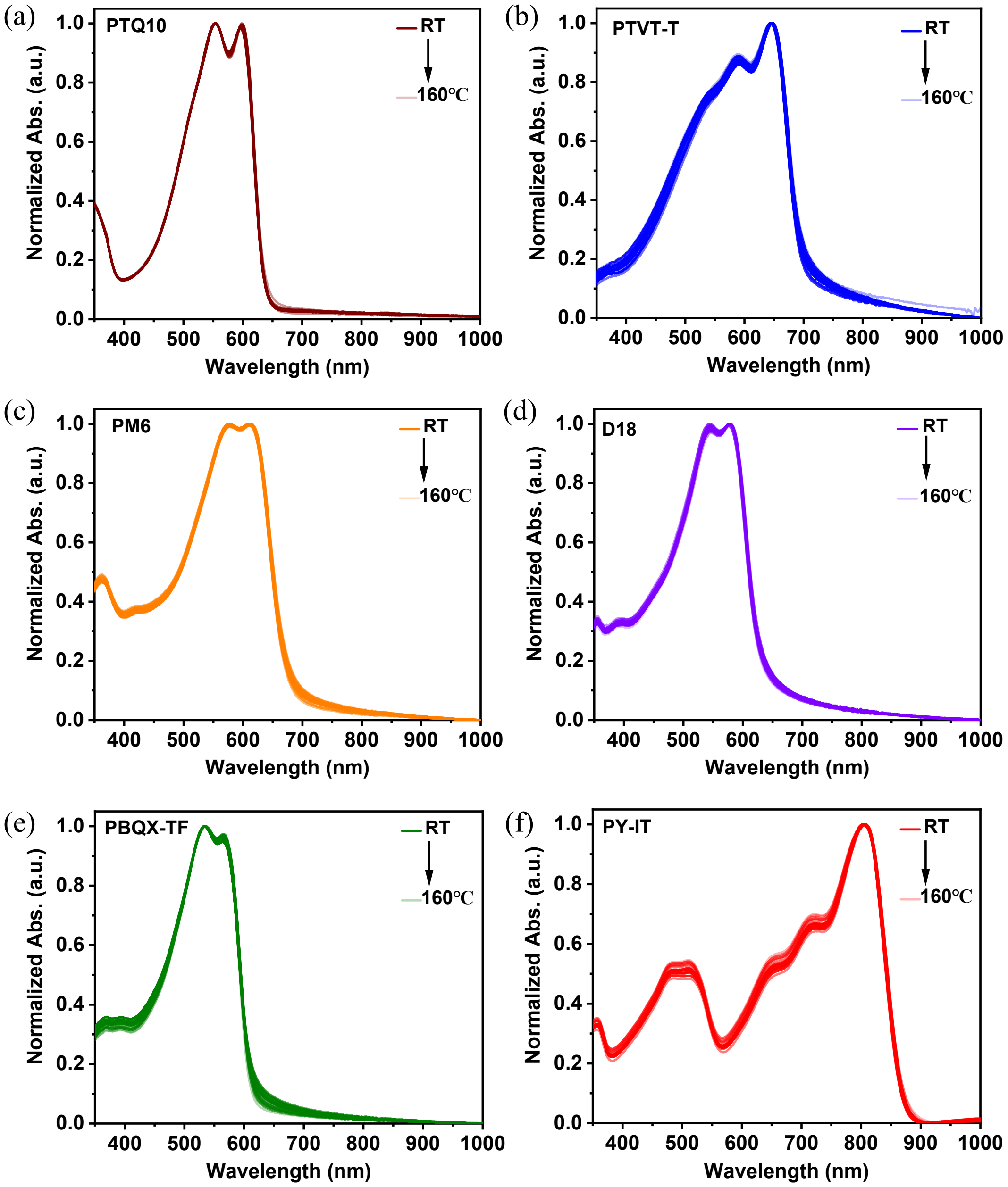

Fig. S12. Temperature-dependent UV-vis absorption spectra of five PDs (a-e) and PY-IT (f) films.

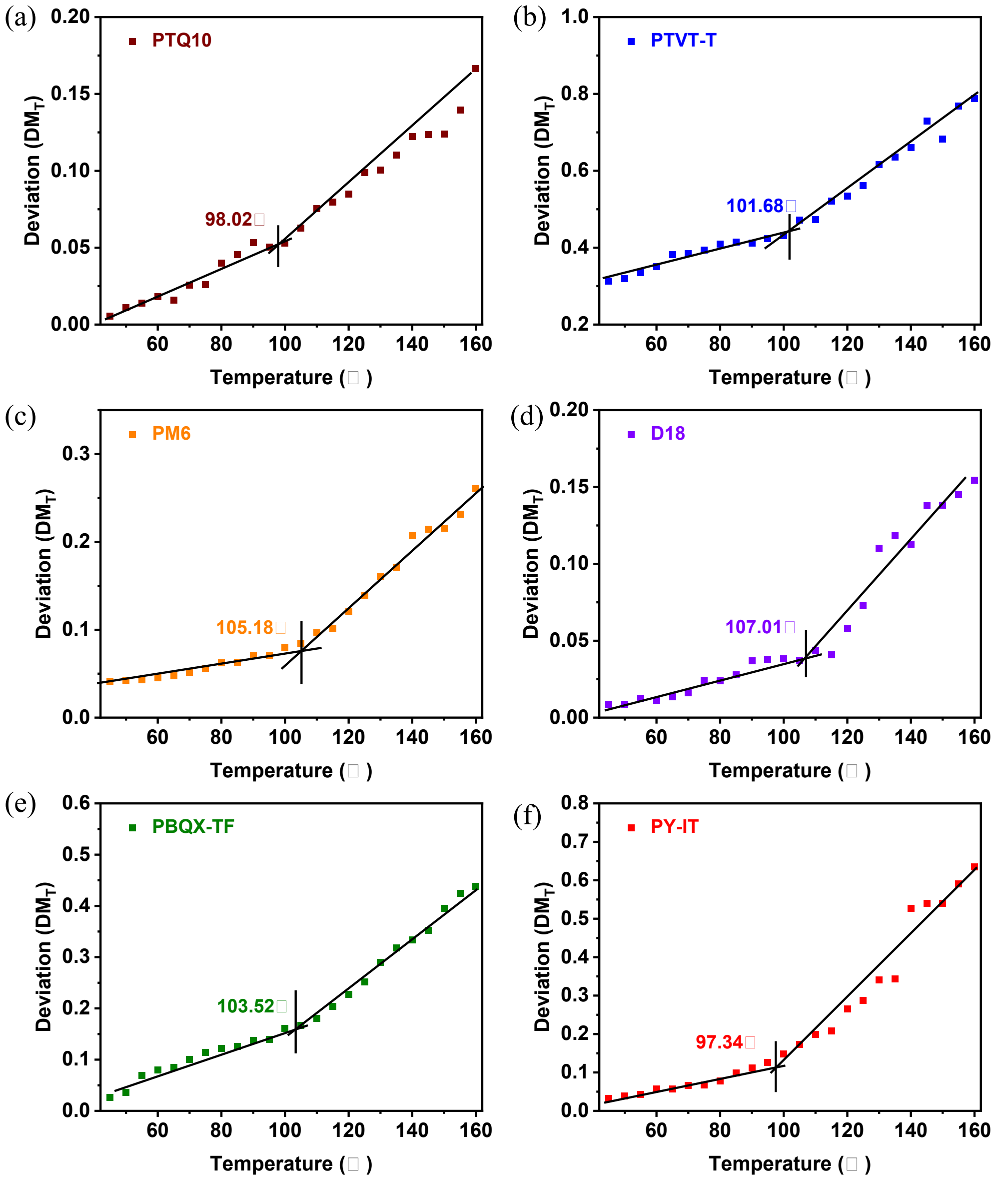

Fig. S13. Plots of the deviation metric (DM$_T$) of five polymer donors (a-e) and PY-IT (f) films as a function of annealing temperature.

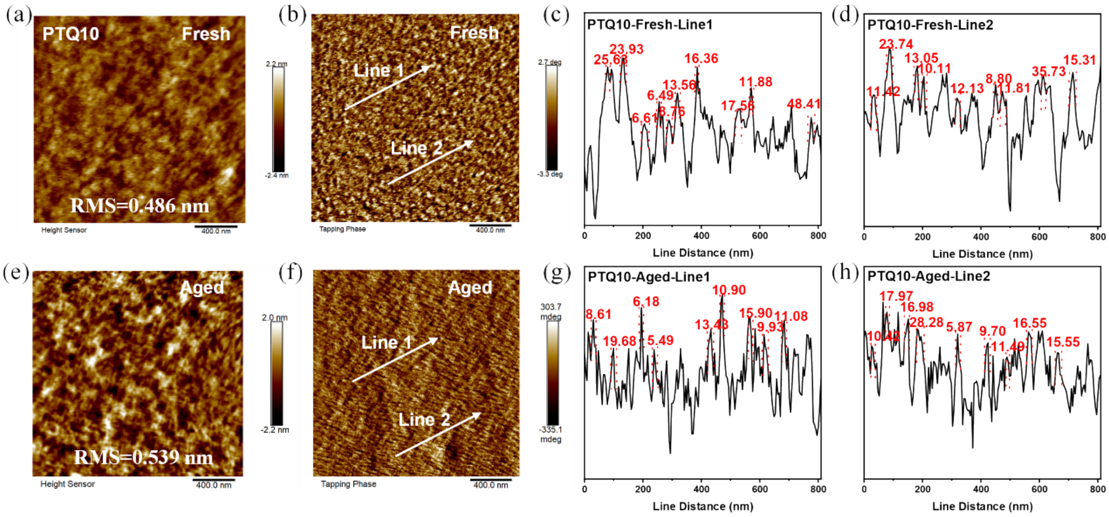

Fig. S14. AFM height, phase images, and line-cut profiles of fresh (a-d) and aged (e-h) films of PTQ10. The fibril width is estimated from the full width at half maximum (FWHM) of the distance between two adjacent dashed lines in the graph.

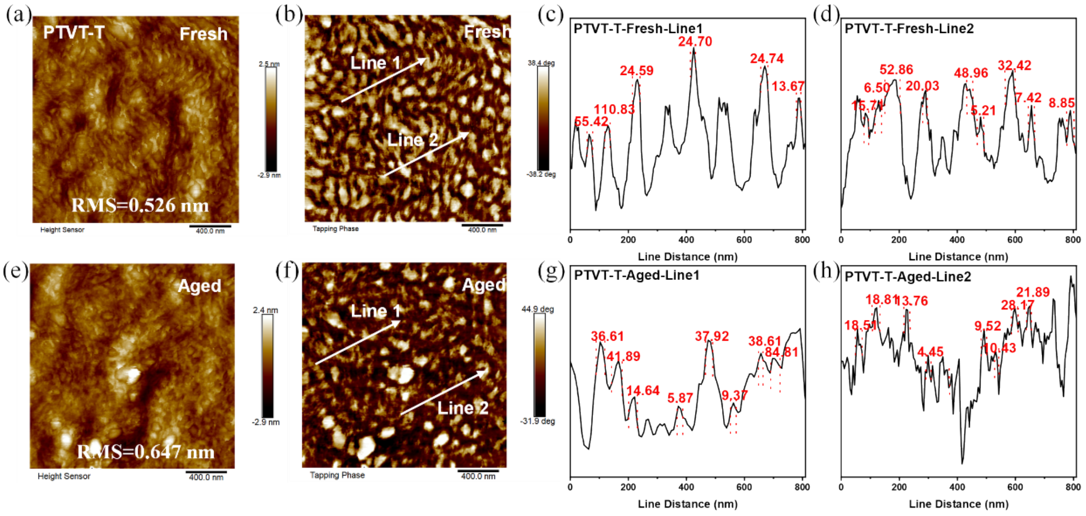

Fig. S15. AFM height, phase images, and line-cut profiles of fresh (a-d) and aged (e-h) films of PTVT-T.

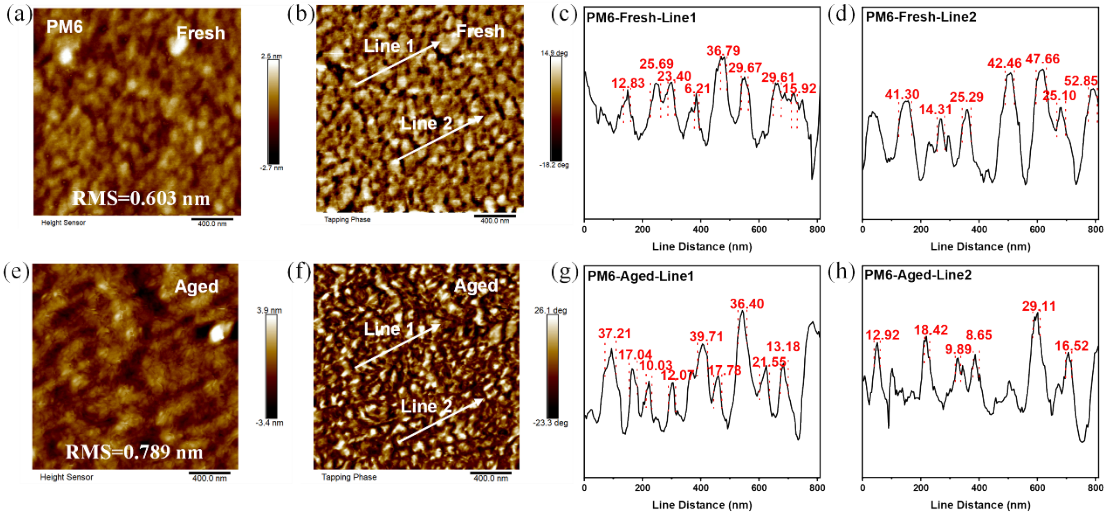

Fig. S16. AFM height, phase images, and line-cut profiles of fresh (a-d) and aged (e-h) films of PM6.

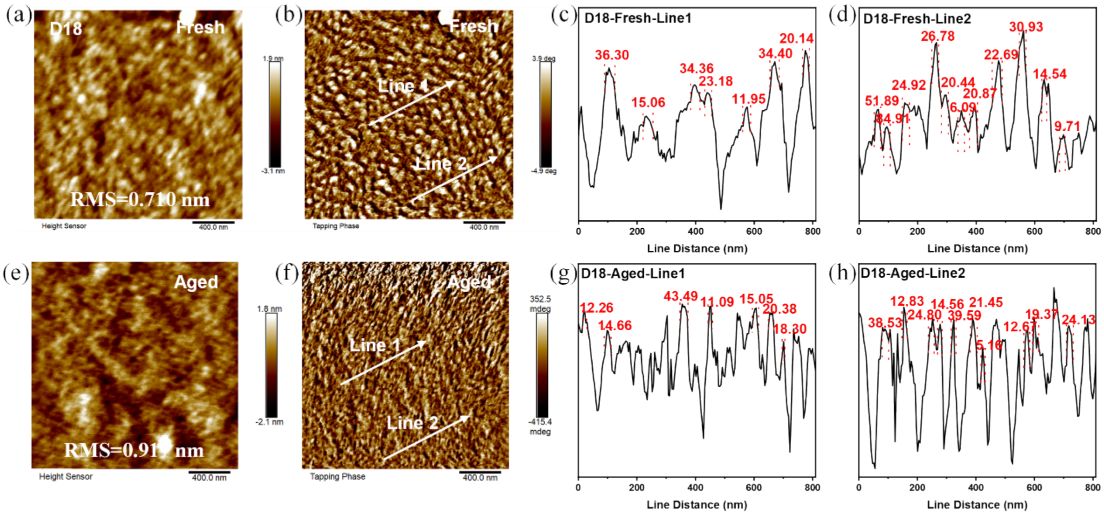

Fig. S17. AFM height, phase images, and line-cut profiles of fresh (a-d) and aged (e-h) films of D18.

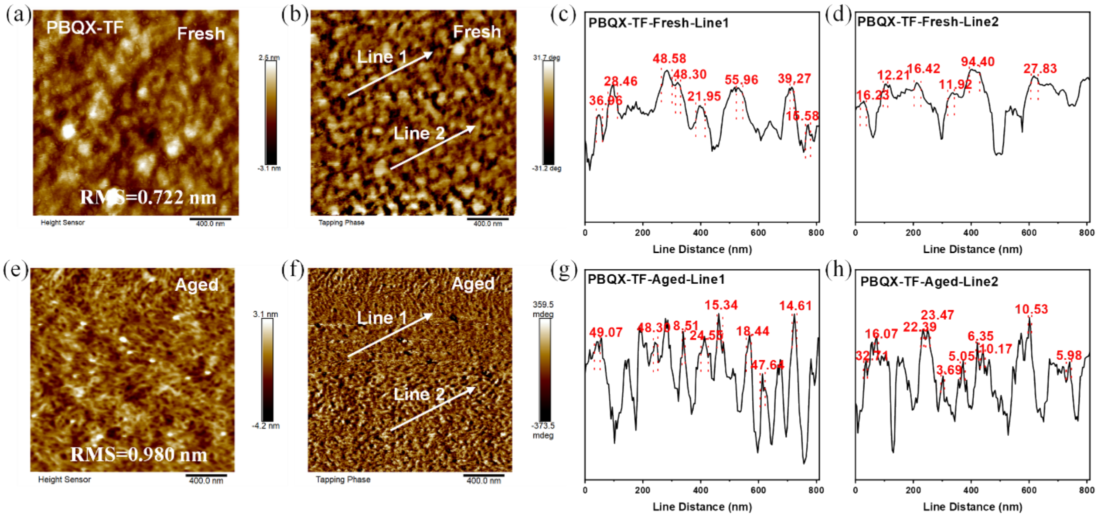

Fig. S18. AFM height, phase images, and line-cut profiles of fresh (a-d) and aged (e-h) films of PBQX-TF.

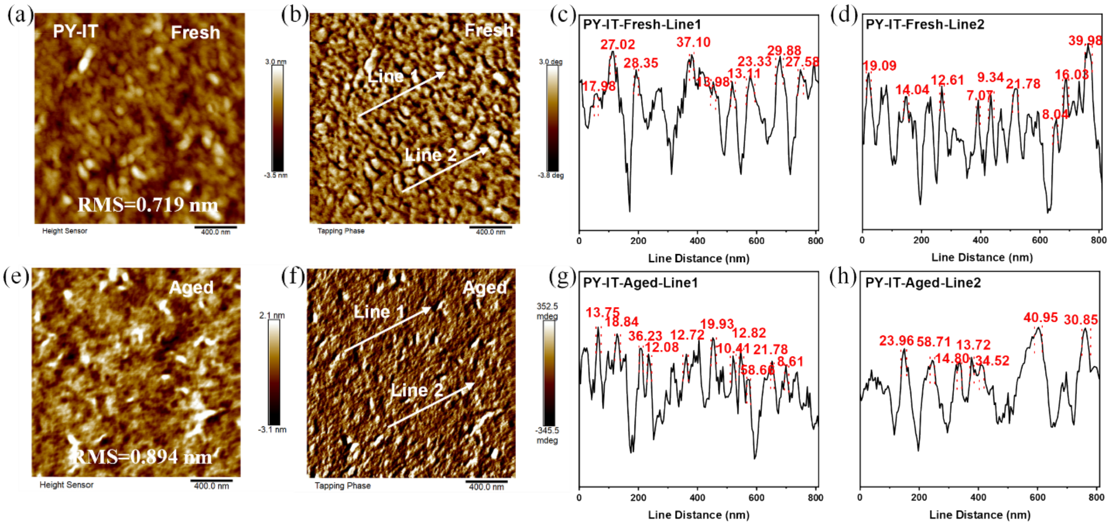

Fig. S19. AFM height, phase images, and line-cut profiles of fresh (a-d) and aged (e-h) films of PY-IT.

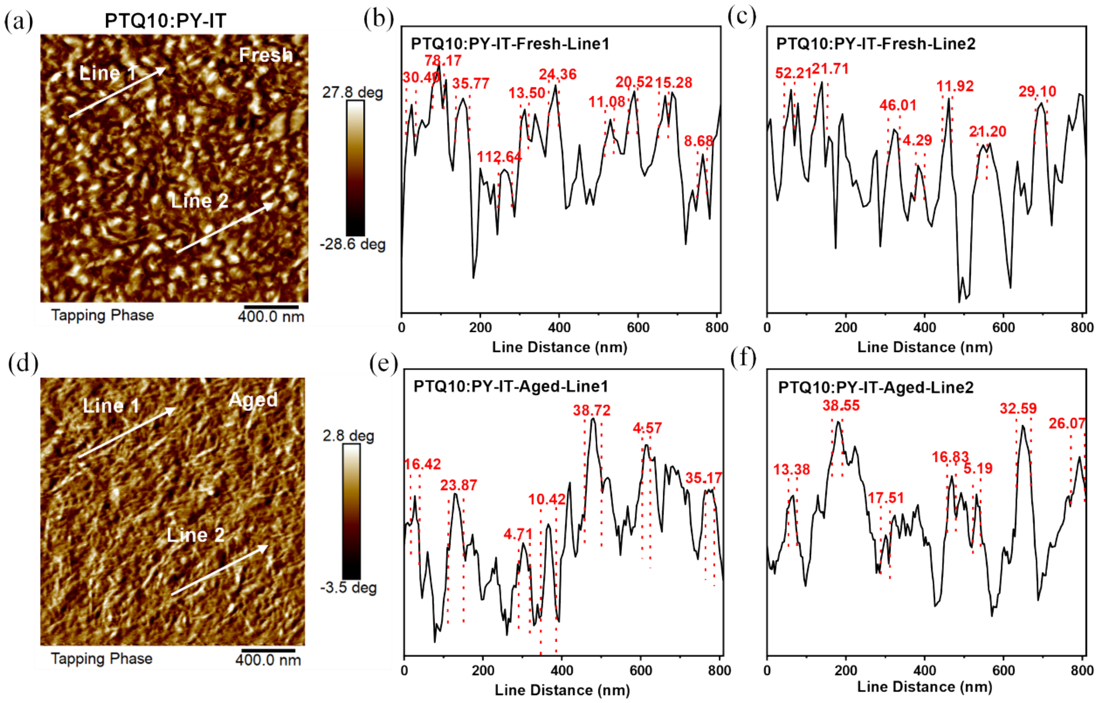

Fig. S20. AFM phase images and line-cut profiles of fresh (a-c) and aged (d-f) films of PTQ10:PY-IT.

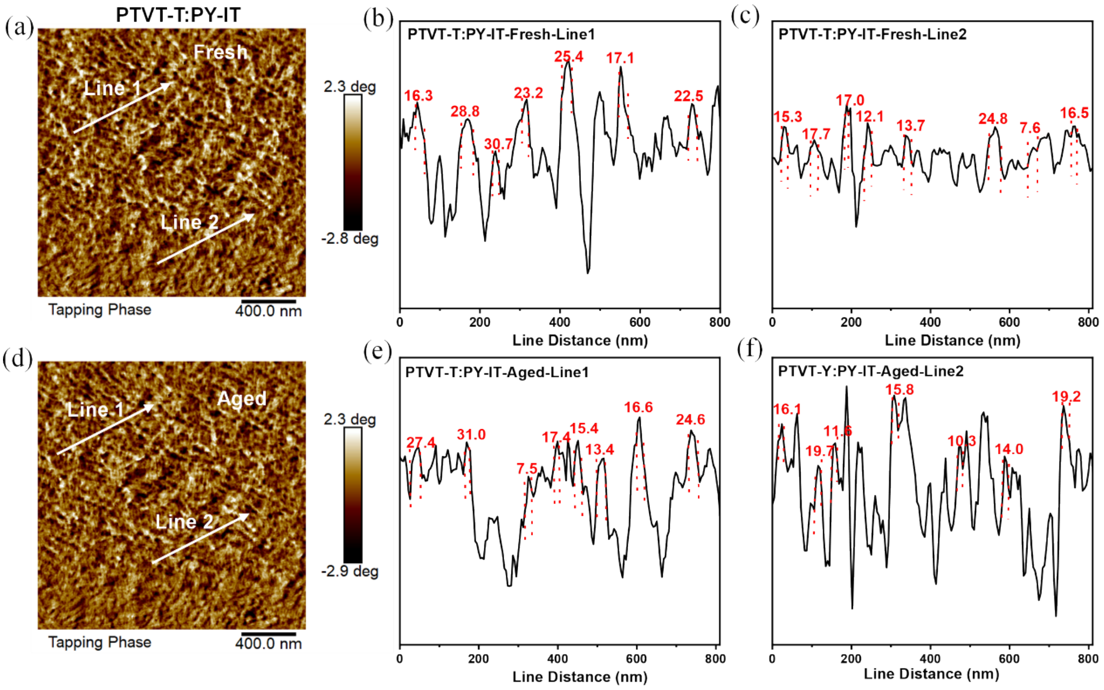

Fig. S21. AFM phase images and line-cut profiles of fresh (a-c) and aged (d-f) films of PTVT-T:PY-IT.

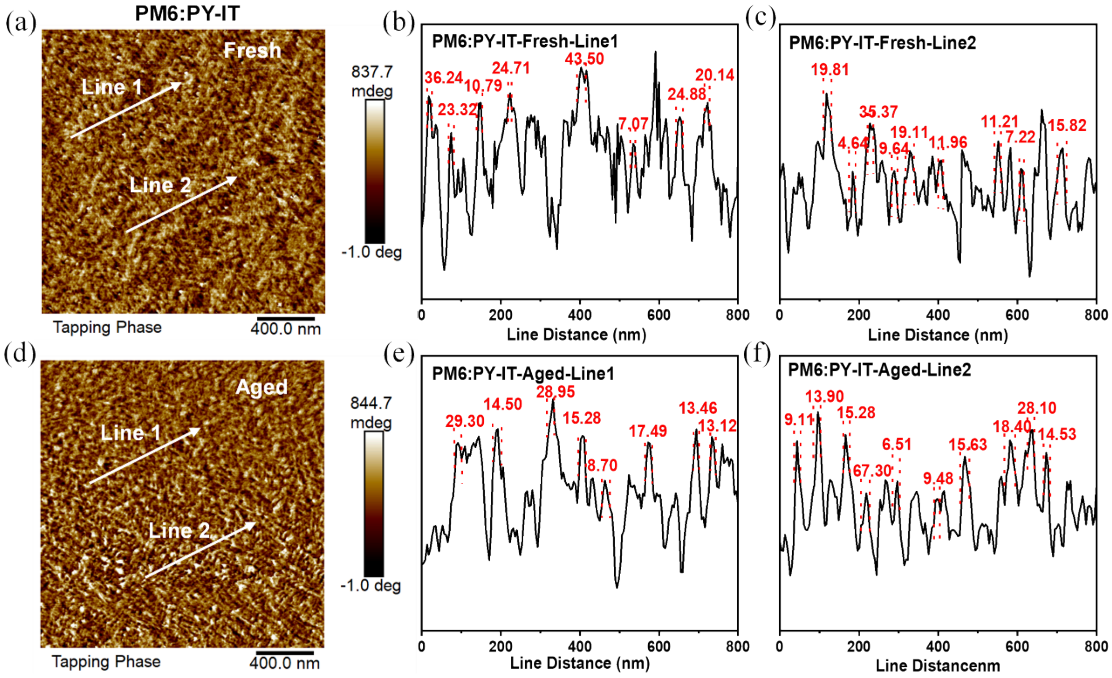

Fig. S22. AFM phase images and line-cut profiles of fresh (a-c) and aged (d-f) films of PM6:PY-IT.

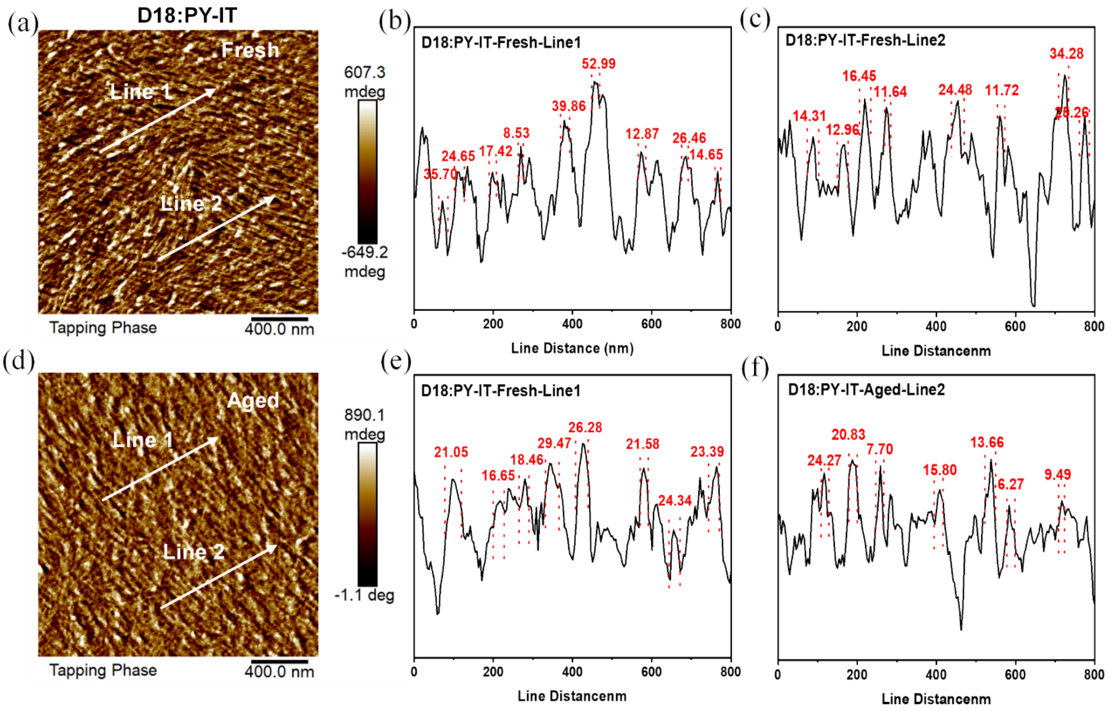

Fig. S23. AFM phase images and line-cut profiles of fresh (a-c) and aged (d-f) films of D18:PY-IT.

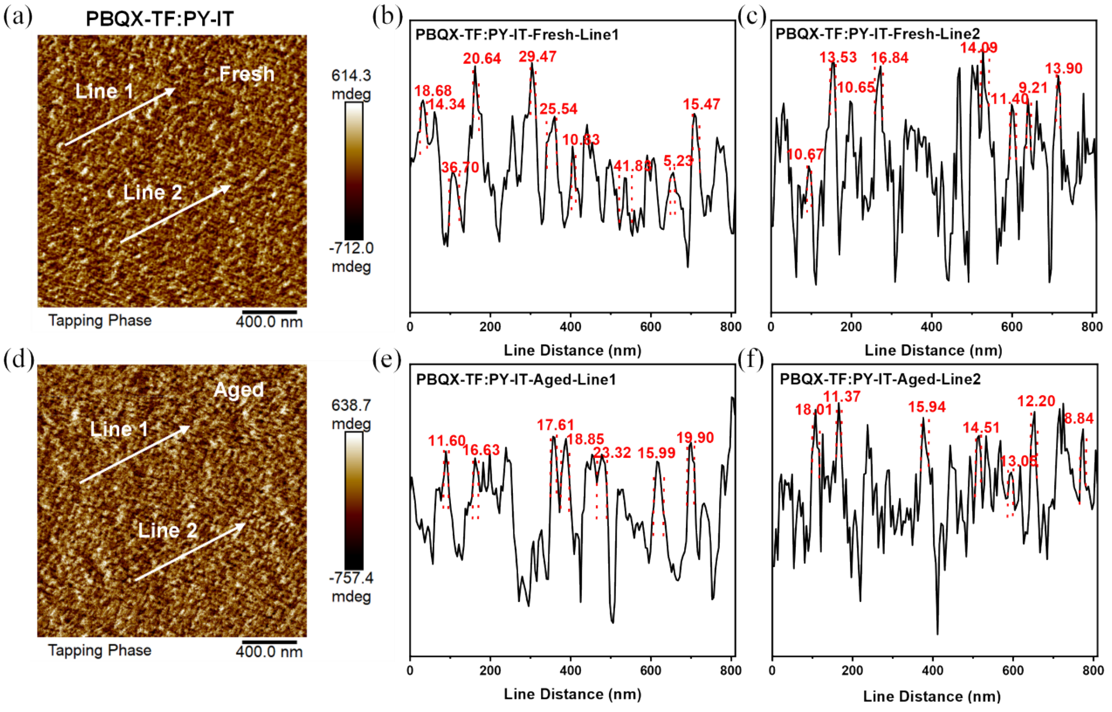

Fig. S24. AFM phase images and line-cut profiles of fresh (a-c) and aged (d-f) films of PBQX-TF:PY-IT.

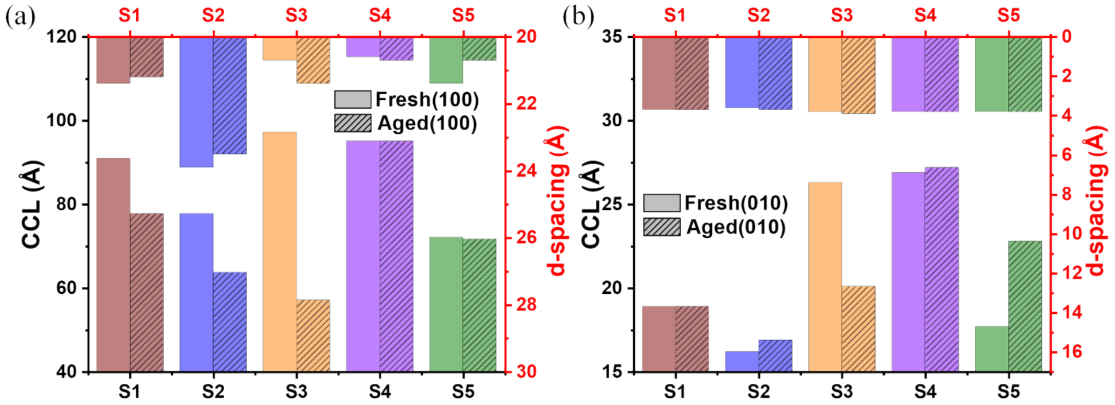

Fig. S25. Extracted CCL and *d*-spacing of (a) IP (100) and (b) OOP (010) scattering peaks fresh and aged blend films (S1: PTQ10:PY-IT, S2: PTVT-T:PY-IT, S3: PM6:PY-IT, S4: D18:PY-IT and S5: PBQX-TF:PY-IT).

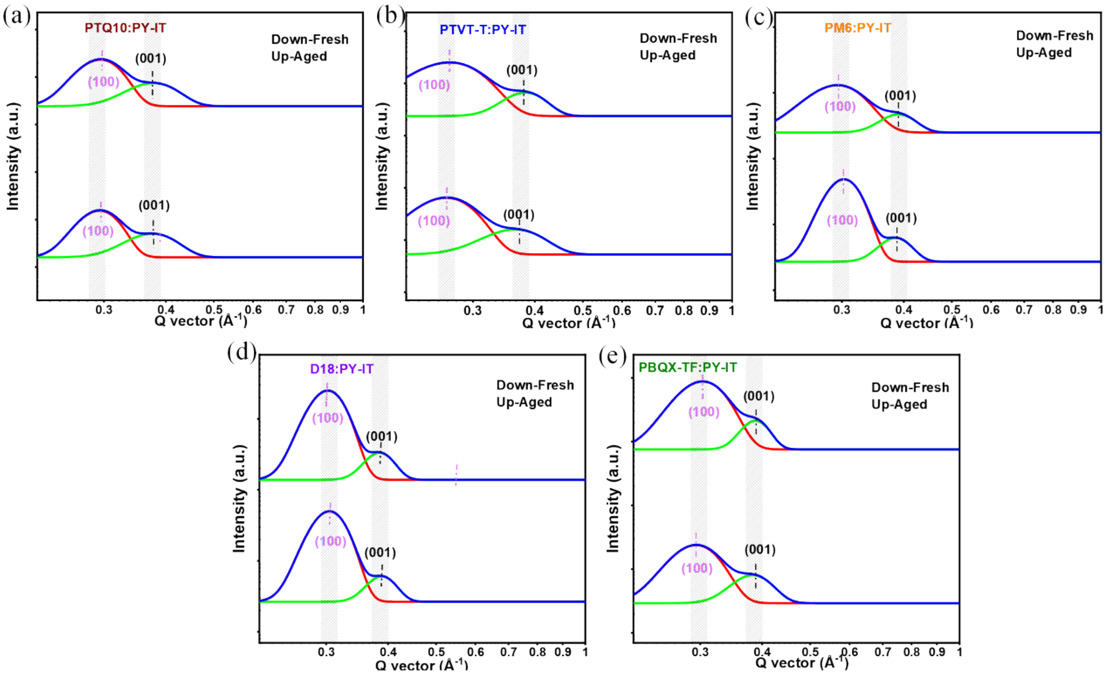

Fig. S26. (a-e) Multiple-peak splitting fits of (100) and (001) peaks in the IP direction for fresh and aged blend films.

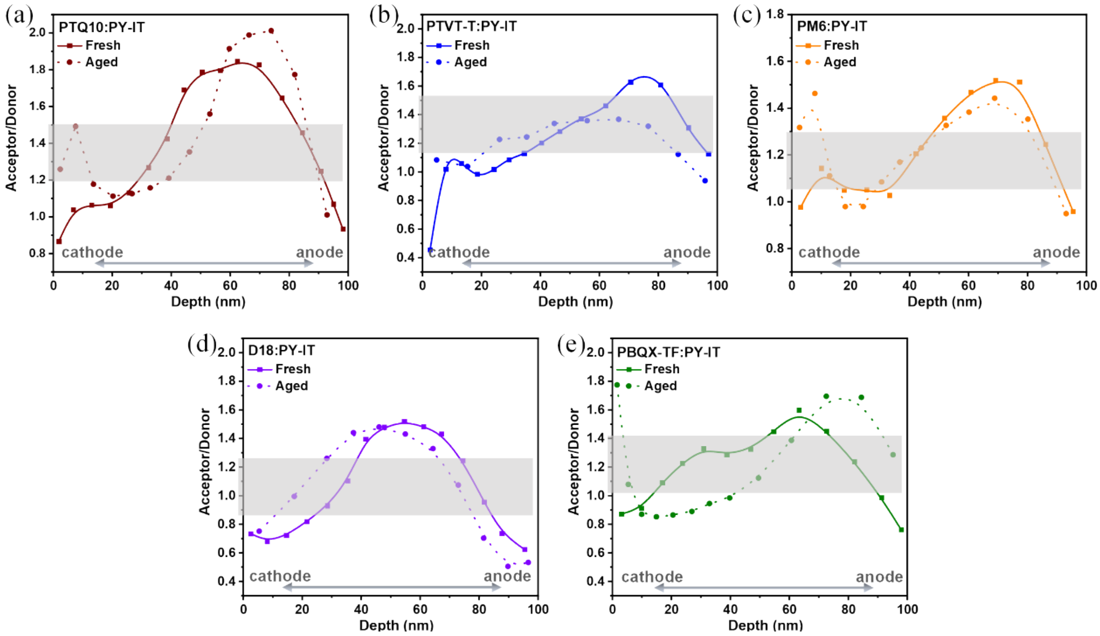

Fig. S27. Compositional distribution of fresh and aged blend films along the depth direction: (a) PTQ10:PY-IT, (b) PTVT-T:PY-IT, (c) PM6:PY-IT, (d) D18:PY-IT and (e) PBQX-TF:PY-IT.

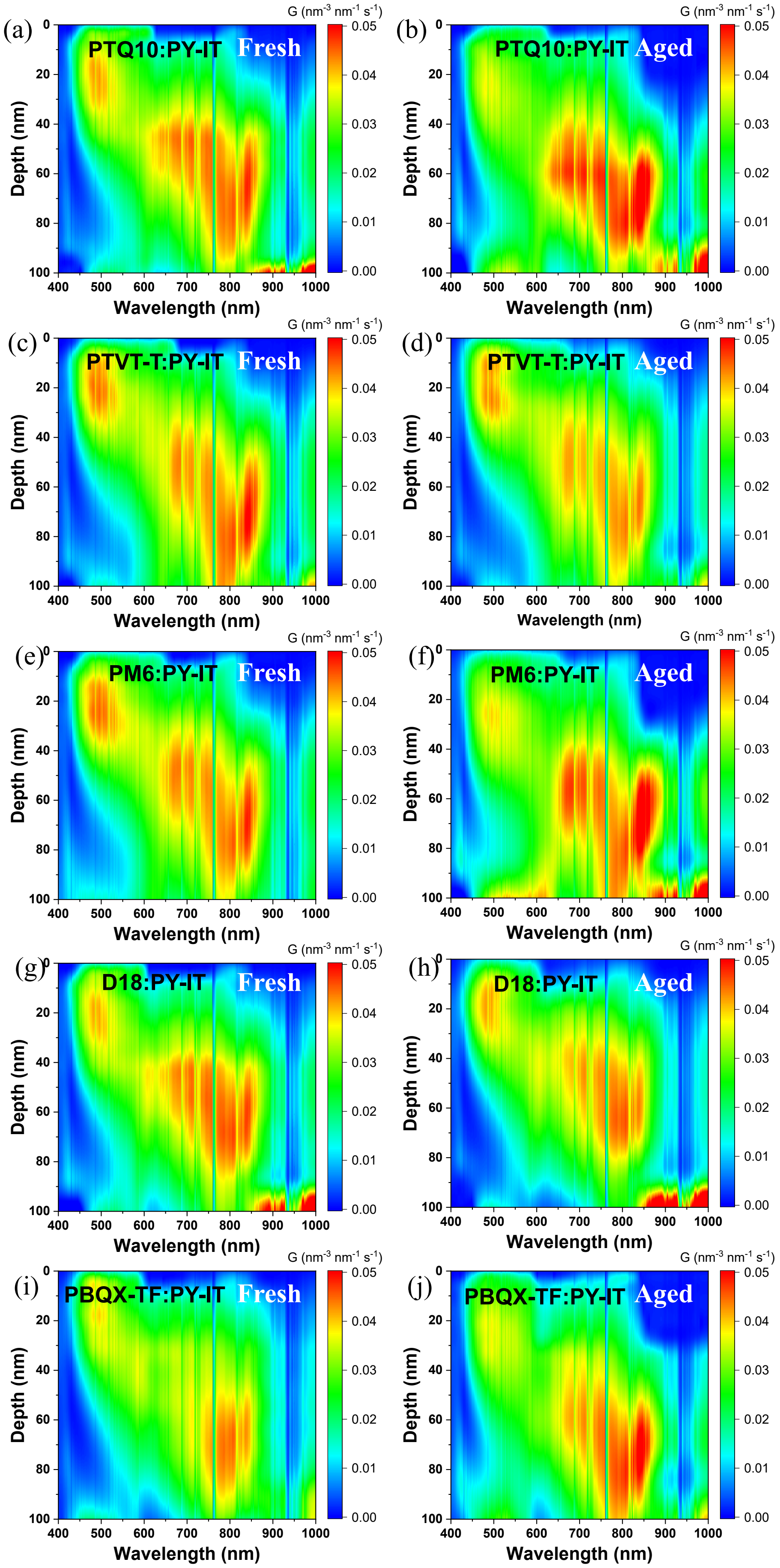
(a)
PTQ10:PY-IT Fresh
(b)
PTQ10:PY-IT Aged
(c)
PTVT-T:PY-IT Fresh
(d)
PTVT-T:PY-IT Aged
(e)
PM6:PY-IT Fresh
(f)
PM6:PY-IT Aged
(g)
D18:PY-IT Fresh
(h)
D18:PY-IT Aged
(i)
PBQX-TF:PY-IT Fresh
(j)
PBQX-TF:PY-IT Aged
Depth (nm)
0
20
40
60
80
100
Wavelength (nm)
400
500
600
700
800
900
1000
G (nm^{-3} nm^{-1} s^{-1})
0.00
0.01
0.02
0.03
0.04
0.05

Fig. S28. Simulated exciton generation contours as a function of film depth for fresh and aged blend films of (a, b) PTQ10:PY-IT, (c, d) PTVT-T:PY-IT, (e, f) PM6:PY-IT, (g, h) D18:PY-IT and (i, j) PBQX-TF:PY-IT.

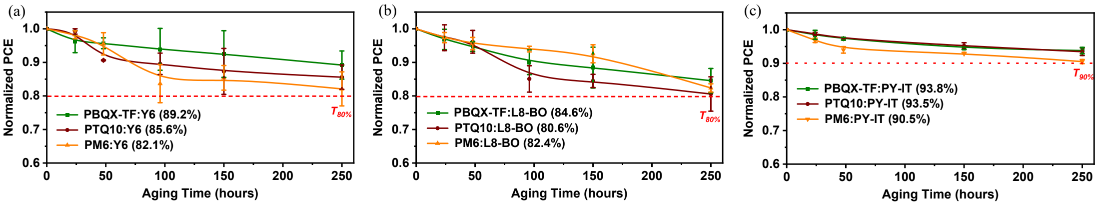

Figure S29. Variation of normalized PCE of devices as a function of the annealing time of (a) PD:Y6, (b) PD:L8-BO and (c) PD:PY-IT active layer under continuous thermal annealing at 80 °C in the nitrogen atmosphere under the dark condition.

Table S1. Photovoltaic parameters of all-PSC devices by varying the thermal aging time at 80 °C.

Active layer	Aged Time (h)	V_{oc} (V)	J_{sc} (mA/cm^2)	FF (%)	PCE (%)[a]
PTQ10:PY-IT	0	0.96	22.12	65.15	13.83 (13.27±0.56)
	24	0.96	21.94	64.87	13.66 (13.00±0.66)
	48	0.96	21.28	64.58	13.19 (12.87±0.32)
	150	0.96	20.76	64.42	12.84 (12.60±0.24)
	250	0.96	20.72	63.28	12.59 (12.41±0.18)
PTVT-T:PY-IT	0	0.86	23.96	74.45	15.34 (15.20±0.14)
	24	0.86	23.84	72.85	14.94 (14.74±0.20)
	48	0.86	23.71	71.82	14.64 (14.50±0.14)
	150	0.86	23.51	71.72	14.50 (14.47±0.03)
	250	0.85	23.09	71.87	14.11 (13.94±0.17)
PM6:PY-IT	0	0.93	25.04	70.81	16.49 (16.25±0.24)
	24	0.93	24.69	70.60	16.21(15.73±0.48)
	48	0.93	23.82	69.43	15.38 (15.27±0.11)
	150	0.93	23.71	68.96	15.21 (15.11±0.10)
	250	0.93	23.60	67.56	14.83 (14.70±0.13)
D18:PY-IT	0	0.94	23.54	74.47	16.48 (15.92±0.56)
	24	0.94	23.50	73.18	16.17 (15.60±0.57)
	48	0.93	23.16	72.96	15.71 (15.12±0.59)
	150	0.93	22.58	72.57	15.24 (14.80±0.44)
	250	0.93	22.38	72.12	15.01 (14.51±0.50)
PBQX-TF:PY-IT	0	0.92	24.67	76.30	17.32 (16.94±0.38)
	24	0.92	24.51	75.57	17.04 (16.60±0.44)
	48	0.92	24.47	74.01	16.66 (16.43±0.23)
	150	0.92	23.76	73.64	16.10 (15.92±0.18)
	250	0.92	23.62	73.59	15.99 (15.89±0.10)

[a] Average value in brackets was obtained from 6 devices.

Table S2. Summary of hole and electron mobilities extracted from the SCLC measurements for fresh and aged devices at 80 ℃ for 250 hours in nitrogen.

Active layer	Aged Time (h)	μ_h [$\times 10^{-4}$ cm^2 V^{-1} s^{-1}]	μ_e [$\times 10^{-4}$ cm^2 V^{-1} s^{-1}]	μ_h/μ_e
PTQ10:PY-IT	0	3.75	3.99	0.94
	250	1.94	3.04	0.64
PTVT-T:PY-IT	0	2.78	3.77	0.74
	250	1.52	2.12	0.72
PM6:PY-IT	0	7.84	6.49	1.21
	250	5.42	3.58	1.51
D18:PY-IT	0	6.36	4.09	1.56
	250	2.54	3.23	0.79
PBQX-TF:PY-IT	0	6.89	6.08	1.13
	250	2.69	4.15	0.65

Table S3. Summary of packing parameters for the fresh and aged films extracted from the GIWAXS measurements.

Position Active Layer	Conditions	Out of plane			In-plane					
		d-spacing (010) (Å)	FWHM (010)	*CCL* (010) (Å)	*d*-spacing (100) (Å)	FWHM (100)	*CCL* (100) (Å)	*d*-spacing (001) (Å)	FWHM (001)	*CCL* (001) (Å)
PTQ10:PY-IT	Fresh	3.70 (1.712 Å^{-1})	0.303	18.9	21.40 (0.294 Å^{-1})	0.062	91.0	16.70 (0.375 Å^{-1})	0.127	44.4
	Aged	3.70 (1.716 Å^{-1})	0.303	18.9	21.20 (0.296 Å^{-1})	0.073	77.8	16.60 (0.378 Å^{-1})	0.114	49.6
PTVT-T:PY-IT	Fresh	3.60 (1.726 Å^{-1})	0.354	16.2	23.90 (0.263 Å^{-1})	0.072	78.6	17.20 (0.365 Å^{-1})	0.148	38.2
	Aged	3.70 (1.712 Å^{-1})	0.339	16.9	23.50 (0.268 Å^{-1})	0.089	63.7	16.40 (0.383 Å^{-1})	0.116	48.6
PM6:PY-IT	Fresh	3.80 (1.649 Å^{-1})	0.217	26.3	20.70 (0.303 Å^{-1})	0.058	97.3	16.30 (0.386 Å^{-1})	0.112	50.5
	Aged	3.90 (1.614Å^{-1})	0.284	20.1	21.40 (0.294 Å^{-1})	0.099	57.1	16.20 (0.389Å^{-1})	0.109	51.9
D18:PY-IT	Fresh	3.80 (1.653 Å^{-1})	0.213	26.9	20.60 (0.305 Å^{-1})	0.060	95.1	16.40 (0.384 Å^{-1})	0.102	55.6
	Aged	3.80 (1.643 Å^{-1})	0.210	27.2	20.70 (0.303 Å^{-1})	0.059	95.1	16.20 (0.388 Å^{-1})	0.095	59.7
PBQX-TF:PY-IT	Fresh	3.80 (1.645 Å^{-1})	0.322	17.6	21.40 (0.293 Å^{-1})	0.078	72.1	16.40 (0.384 Å^{-1})	0.097	58.5
	Aged	3.80 (1.640 Å^{-1})	0.250	22.8	20.70 (0.304 Å^{-1})	0.079	71.7	16.20 (0.389 Å^{-1})	0.082	69.0

References

1. J. Jang, J. Kim, S. Lee, C.-M. Oh, I.-W. Hwang, S. Kim, A. Park, D. Kang, C. Jang, T. Ki, H. Kim and K. Lee, *ACS Appl. Energy Mater.* 2023, **6**, 9778.
2. W. Ma, J. R. Tumbleston, M. Wang, E. Gann, F. Huang and H. Ade, *Adv. Energy Mater.* 2013, **3**, 864.
3. T. Chen, Y. Zhong, T. Duan, X. Tang, W. Zhao, J. Wang, G. Lu, G. Long, J. Zhang, K. Han, X. Wan, B. Kai and Y. Chen, *Angew. Chem., Int. Ed.,* 2025, **137**, e202412983.
4. E. A. Katz, A. Mescheloff, I. Visoly-Fisher and Y. Galagan, *Sol. Energy Mater. Sol. Cells.* ,2016, **144**, 273.
5. P. W. M. Blom, V. D. Mihailetchi, L. J. A. Koster and D. E. Markov, *Adv. Mater.,* 2007, **19**, 1551.
6. E. A. Katz, D. Faiman, S. M. Tuladhar, J. M. Kroon, M. M. Wienk, T.Fromherz, F. Padinger, C. J. Brabec, and N. S. Sariciftci, *J. Appl. Phys.,* 2001, **90**, 5243.